Title
COMBUSTION OF LEAN MIXTURES UNDER SIMULATED INTERNAL COMBUSTION ENGINE CONDITIONS

Authors
Dunn-Rankin, D.
Sawyer, R.F.

Publication Date
1983-10-01

LBL-16745 c.2

Lawrence Berkeley Laboratory

UNIVERSITY OF CALIFORNIA

APPLIED SCIENCE DIVISION

To be presented at the Fall Meeting of the Western States Section/The Combustion Institute, University of California at Los Angeles, CA, October 17, 1983

COMBUSTION OF LEAN MIXTURES UNDER SIMULATED INTERNAL COMBUSTION ENGINE CONDITIONS

D. Dunn-Rankin and R.F. Sawyer

October 1983

APPLIED SCIENCE DIVISION

Prepared for the U.S. Department of Energy under Contract DE-AC03-76SF00098

DISCLAIMER

LBL-16745 c.2

Lawrence Berkeley Laboratory

UNIVERSITY OF CALIFORNIA

APPLIED SCIENCE DIVISION

To be presented at the Fall Meeting of the
Western States Section/The Combustion Institute,
University of California at Los Angeles, CA,
October 17, 1983

COMBUSTION OF LEAN MIXTURES UNDER SIMULATED INTERNAL COMBUSTION ENGINE CONDITIONS

D. Dunn-Rankin and R.F. Sawyer

October 1983

APPLIED SCIENCE
DIVISION

Prepared for the U.S. Department of Energy under Contract DE-AC03-76SF00098

WSS/CI Paper No. 83-53

COMBUSTION OF LEAN MIXTURES UNDER SIMULATED INTERNAL COMBUSTION ENGINE CONDITIONS

D. Dunn-Rankin and R.F. Sawyer

Mechanical Engineering Department and
Applied Science Division, Lawrence Berkeley Laboratory
University of California
Berkeley CA 94720

This work was supported by the Assistant Secretary for Conservation and Renewable Energy, Office of Transportation Programs, Division of Transportation Energy of the U.S. Department of Energy under contract number DE-AC03-76SF00098.

ABSTRACT

An experimental study is made of fuel lean combustible gases inside a square cross-section enclosure fitted with a reciprocating piston. The piston is pneumatically driven and simulates the compression-expansion phase of internal combustion engine operation. Intake and exhaust valving is not included. Two borosilicate glass windows provide full optical access to the enclosure. A line igniter produces an approximately two-dimensional flame front. Flame location and shape are obtained from high speed schlieren and shadowgraph movies. Pressure measurements and piston location records are simultaneously acquired. Mass burning rate is calculated from flame location, piston location, and pressure information.

The experiments concentrate on lean fuel/air mixture behavior. Situations investigated are:

1) Compression followed by combustion

2) Compression-expansion-combustion

Compression-combustion experiments investigate the effect of equivalence ratio and ignition time on combustion at higher than atmospheric pressure. A piston generated "roll-up vortex" is observed from the movies. The mass burning rate is not noticeably affected when the flame interacts with the "roll-up vortex".

Compression-expansion-combustion experiments explore the phenomenon of flame propagation during piston expansion. Three types of flame propagation are observed. Type 1:

Flames propagate rapidly enough to burn the mixture before the piston is fully expanded. Type 2: Flames begin to propagate as in Type 1 but the mass burning rate decreases as the chamber expands. Type 2 flames propagate normally again once the piston slows near its full expansion. Type 3: The flame is quenched during the expansion.

Equivalence ratio is the most significant factor in determining flame propagation behavior.

INTRODUCTION

This investigation is part of a study of the fundamental processes important to the combustion of lean homogeneous mixtures in reciprocating internal combustion engines. Flame propagation in engines is affected by wall interactions, combustion chamber dynamics, in-cylinder fluid mechanics, and equivalence ratio. Lean mixtures are of particular interest because lean combustion is a promising approach for the improvement of fuel economy and reduction of emissions (Dale and Oppenheim, 1982). However, the application of lean combustion to engines still encounters difficulties related to ignition reliability, combustion rate reduction, and increased hydrocarbon emissions (Shiomoto, et al., 1978; Naguchi, et al., 1976). Characterization of lean mixture burning rate reduction in simulated reciprocating engine combustion is the subject of this work.

Experiments are conducted in a square cross section cylinder with a reciprocating piston. The square cross section allows the use of flat windows as side walls. In-cylinder fluid motion is limited to piston and flame generated flow. This motion is small and allows the flame to be approximated as a laminar deflagration wave. In previous studies the effects of fuel type and equivalence ratio on constant volume flame propagation were explored (Woodard et al., 1981; Steinert et al., 1982). Flame propagation near the lean limit in an expanding chamber, without prior compression, has also been studied (Smith et al., 1979). Two situations are investigated. 1) Compression followed by a constant volume combustion and 2) Compression followed by expansion, with combustion during the expansion stroke. Slow burning lean mixtures are expected to burn into the expansion stroke in a real engine. The compression-expansion-combustion experiments characterize lean mixture, expansion stroke combustion.

EXPERIMENTAL APPROACH

Measurements are made in the compression-expansion mode of a rapid compression apparatus (CE-1) which is designed to provide full optical access to combustion events simulating those occurring in reciprocating internal combustion engines. Relevant features of the apparatus are described here; a more detailed description may be found in Oppenheim et. al. (1976) and Smith (1977).

The experimental apparatus and instrumentation are represented schematically in Figure 1. The test section consists of a square cross-section (38mm x 38mm) combustion chamber fitted with a pneumatically driven piston. The two

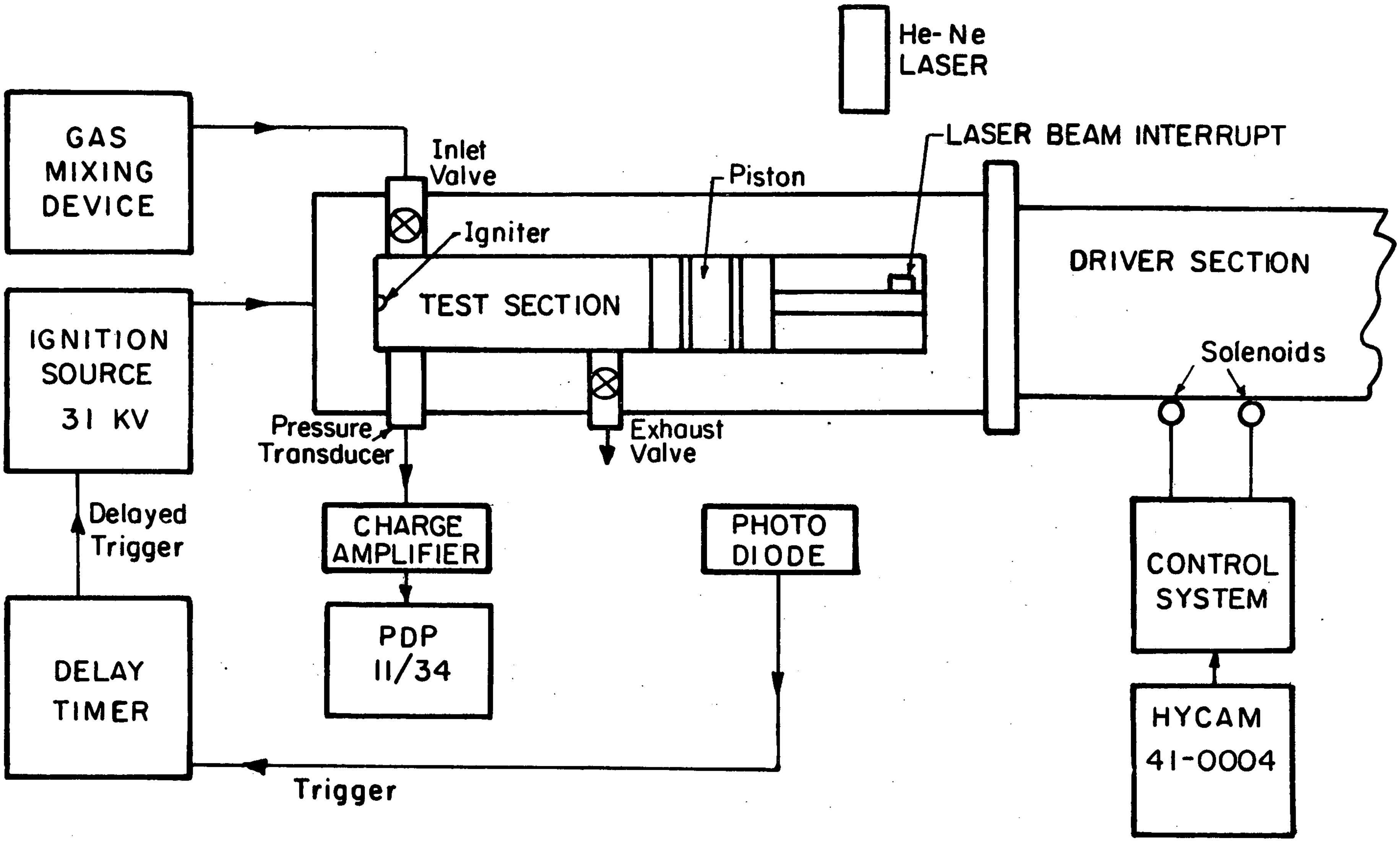

Figure 1. Schematic of experimental apparatus.

vertical sides of the combustion chamber are optical quality borosilicate glass windows. The top and bottom walls are stainless steel, fitted with instrument ports. The piston is sealed with two teflon rings. The endwall opposite the piston contains a line ignition source.

The fuel/air mixture is delivered by a gas mixing device which controls the equivalence ratio by flow rotameters. The rotameters were calibrated with soap bubble meters. The uncertainty in the equivalence ratio is about 5%. Before each experiment the chamber is flushed for the equivalent of 20 complete changes of gas mixture to insure uniform mix without residual gas.

The line ignition source consists of a row of five 1.5 mm spark gaps. The spark gaps run in a horizontal row from window to window. The line igniter is designed to produce flame uniformity in the direction perpendicular to the windows. The ignition energy comes from a 130 picofarad capacitor charged to approximately 45 kV. The stored energy is dissipated in a triggered spark gap (EG&G GP32B) and across the line igniter. The ignition energy in terms of stored energy is 130 millijoules. Approximately 60% of the stored energy reaches the line igniter.

The propagation of the flame into the unburned mixture is recorded with a high speed schlieren system in a Z-configuration, Figure 2, using two concave mirrors of 3.94 m focal length. The combination of a point light source (Oriel xenon lamp, model 6140, at 20-25 amps with a 2.0 mm hole) and the first mirror provide parallel light through the test

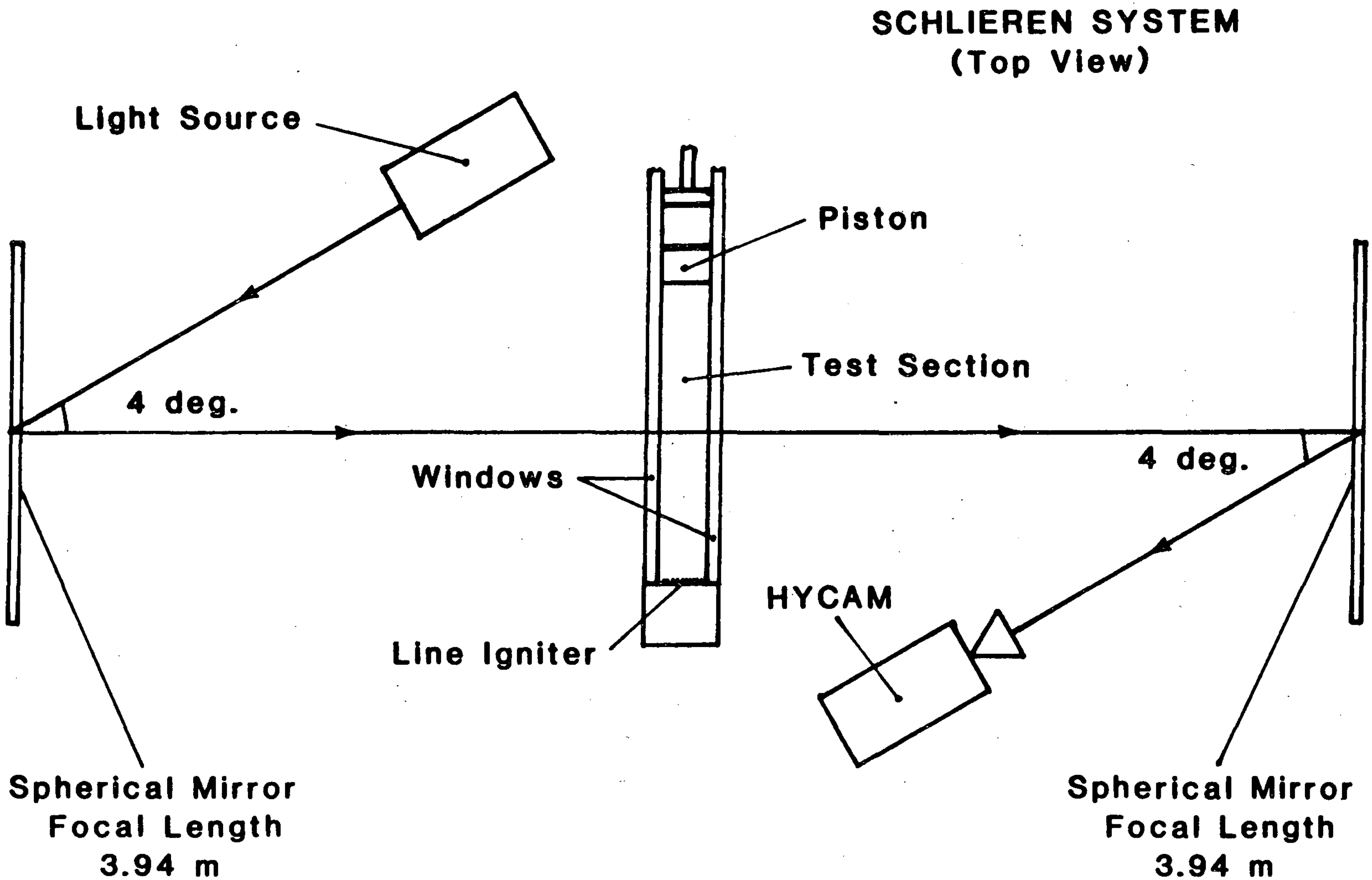

XBL 818-1741

Figure 2. Schematic of schlieren system.

section. This light is focused at a vertical schlieren knife edge stop by the second mirror and imaged at the film plane of a high speed 16 mm camera (Hycam Model 41-0004, about 5400 frames/s, Kodak Tri-X-Reversal film).

The chamber pressure is measured using a piezoelectric transducer (AVL 120P300 cvk#1402, sensitivity 42.04 pc/bar) located in the lower front access port just below the igniter. The transducer signals are amplified by a charge amplifier (Kistler 5004E). The pressure data are sampled every 50 microseconds by a PDP 11/34 computer using an AR-11 analog to digital converter. The computer and the charge amplifier are connected through an optical isolator to protect the computer from harmful ground loops and peak currents caused by the igniter.

The piston is driven by compressed air acting on a connected driver piston. The acceleration is controlled by a snubber piston passing through a series of oil filled orifices. The compression-expansion behavior of the apparatus is shown in Figure 3. The chamber length is initally 150 mm. The complete compression stroke contracts the chamber to 18.8 mm (compression ratio 8:1). The compression occurs in three stages. First there is an initial contraction of 4-5 mm. This is followed by a rapid compression to a chamber length of 23.8 mm (6.4:1 volume ratio) and a subsequent bounce back to a chamber length of 26 mm (5.8:1 volume ratio). Although the bounce changes the chamber length by approximately two millimeters, it has a

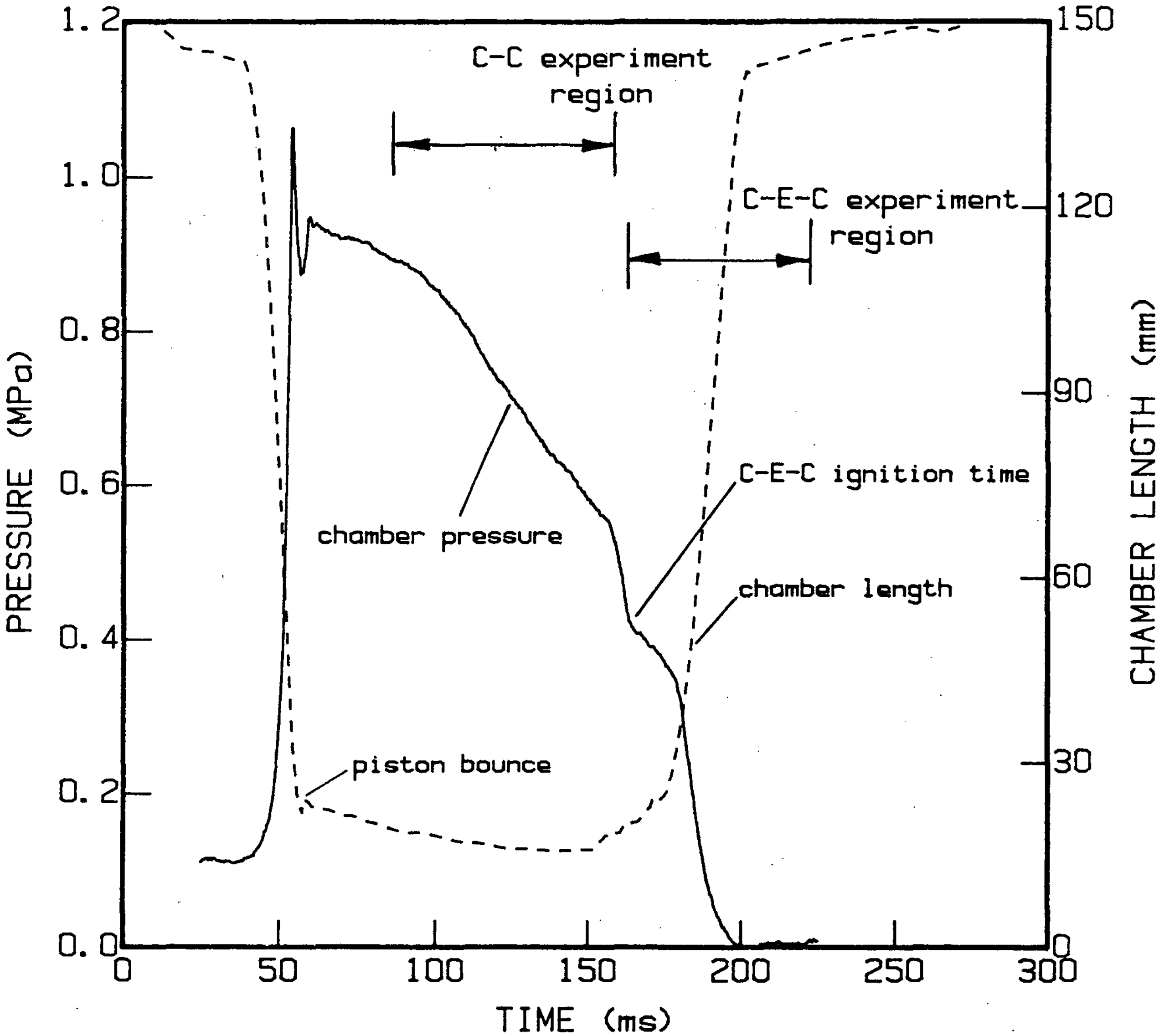

Figure 3. Piston displacement and chamber pressure of the CE-1 apparatus without combustion. C-E-C refers to compression-expansion-combustion experiments. C-C refers to compression combustion experiments.

dramatic effect on the chamber pressure, Figure 3. The pressure drop is approximately equal to the pressure drop predicted by an isentropic expansion analysis. Following the bounce there is a slow compression of 7.2 mm to the final chamber length of 18.8 mm (final volume ratio 8:1). The slow compression takes approximately 50 ms, Figure 3. After the compression the piston remains at top dead center (TDC) for another 50 ms until the driver compression air can be exhausted and the driver air re-introduced for the expansion stroke. The expansion stroke also occurs in three stages. There is an initial false start expansion of 5-6 mm back to a chamber length of approximately 23.5 mm (volume ratio 6.3:1). As in the case of the piston bounce, the initial expansion has a large effect on the chamber pressure due to the small chamber volume. The initial expansion is followed by a short pause and then a rapid expansion back to near bottom dead center (BDC). Finally there is a slow expansion back to true BDC. The complicated piston compression-expansion behavior is surprisingly repeatable. The experiments are conducted during periods when the anomalous piston behavior will have little effect, Figure 3. Ignition is timed to occur either during the pause at TDC, when the driver air is being exhausted, or at the start of the rapid expansion phase. This minimizes piston bounce and false start expansion effects.

The measurements are initiated by the high speed camera. When the camera reaches operating speed a start pulse is sent to the data acquisition system and to the compressed driver air solenoids. When the piston reaches near the bounce point on its primary compression stroke a laser beam is broken beginning the ignition timing sequence. After an operator specified delay interval the line igniter is fired.

With the above described apparatus, compression-expansion-combustion experiments are conducted which involve simultaneously measuring the pressure and photographing both the flame and the piston. In all measurements the initial conditions are atmospheric pressure and ambient temperature. Methane (99.99%) is used as fuel with air as oxidizer. Experiments are conducted at six different lean equivalence ratios (0.61, 0.65, 0.71, 0.76, 0.83, 0.88).

COMPRESSION-COMBUSTION

The compression-combustion experiments consist of constant volume combustion at elevated pressure and temperature. Combustion during compression is not analyzed due to the complication of the piston bounce phenomenon.

Figure 4a shows a typical compressed volume flame propagation sequence. The time of each frame in the sequence is normalized to the total combustion time. The flame expands in semi-cylindrical shape until the wall effects are felt. The flame then molds to the form of the walls. The flame appears always laminar despite the existence of the piston induced "roll-up vortex" (Oppenheim et al., 1976). It has been suggested (Matekunas, 1978) that the "roll-up vortex" has little effect on the combustion process except very near the wall. In the present apparatus, the effect of

a) Typical flame propagation. t* is the total combustion time.

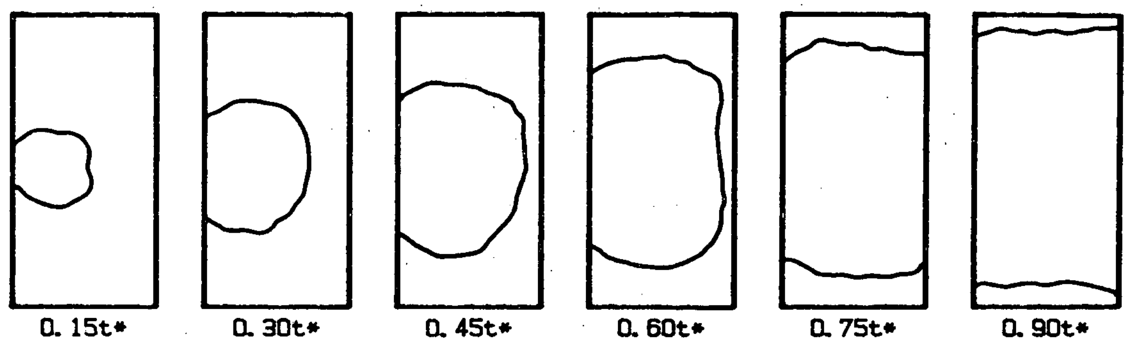

b) Compression-combustion with 17.6 ms ignition time.

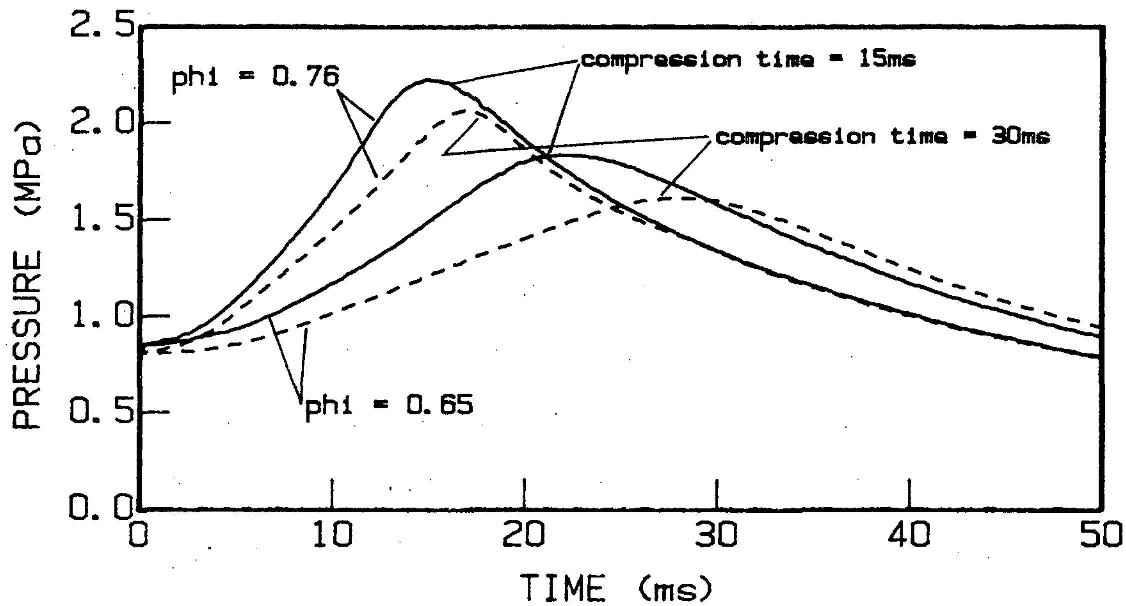

c) Compression-combustion with 40.8 ms ignition time.

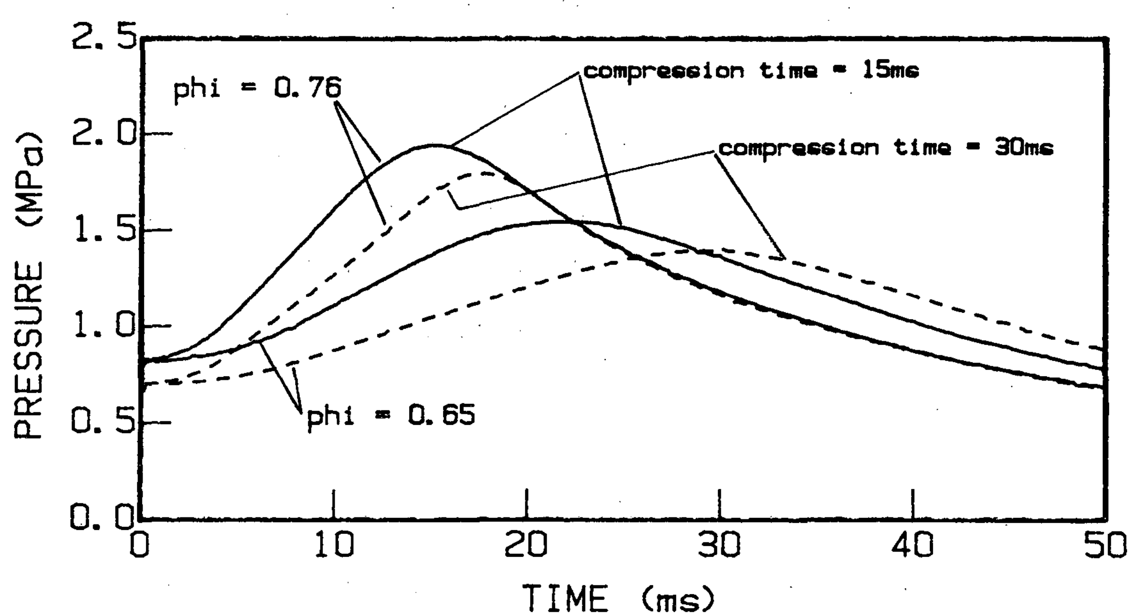

Figure 4. Chamber pressure for compression-combustion. phi denotes equivalence ratio.

piston generated turbulence on the flame propagation near the wall is obscured by thin layers of crevice gas escaping into the compression chamber during the piston bounce. However, the "roll-up vortex" does not appear to affect significantly the measurable combustion related quantities.

The behavior of the pressure in compression-combustion experiments depends on the compression time, the time of ignition and the equivalence ratio. For compression-combustion experiments the ignition time is measured from the time of the compression pressure spike during the piston bounce, Figure 3. The time of ignition in the compression-combustion experiments is substantially different from the ignition timing in a reciprocating engine. The peak pressure spike is chosen as ignition time zero because it provides a convenient time correlation marker between the high speed movies and the pressure data. Figure 4b and Figure 4c show pressure curves for 17.6 ms and 40.8 ms ignition times respectively. The figures show only the combustion portion of the compression-combustion event. The combustion time zero occurs at ignition. In each figure the results from two driving pressures (350 kPa, 550 kPa) and two equivalence ratios (0.65, 0.76) are reported. The drive pressure controls the time required for compression. The two drive pressures are equivalent to 15 ms and 30 ms compression times respectively.

The peak pressure is a strong function of equivalence ratio and a somewhat weaker function of ignition time and compression time. Lower equivalence ratios lead to lower peak pressures as the combustion energy per unit volume is reduced. The depression of peak pressure with longer ignition time comes from the longer time available for mass leak. The leak reduces the available combustion enthalpy. The same is true of the effect of longer compression time.

The time to peak pressure is also strongly dependent on equivalence ratio. The effect of equivalence ratio on ignition time comes from the reduced laminar flame speed at lower equivalence ratios. There is also a correlation between the compression time and the time to peak pressure. The effect of the compression time on the time to peak pressure may be fluid mechanical. Shorter compression time means higher piston speed and a greater amount of piston induced turbulence. The higher turbulence shortens the mass burning time somewhat. The time of ignition has virtually no effect on the time to peak pressure.

Compression-Combustion: effect of ignition time

The effect of the time of ignition on the combustion process at compressed volume is shown in Figure 5. Figure 5a displays the pressure history of six different ignition times (17.6 ms, 40.8 ms, 70.4 ms, 80.0 ms, 90.0 ms, 95.4 ms) at a single equivalence ratio (0.65) and compression time (15 ms). Figure 5b plots the peak pressure and time to peak pressure versus the ignition time. The same trends as noted in Figure 4 are seen. The time to peak pressure is nearly independent of the time of ignition. The peak pressure decreases non-

a) Chamber pressure for six ignition times.

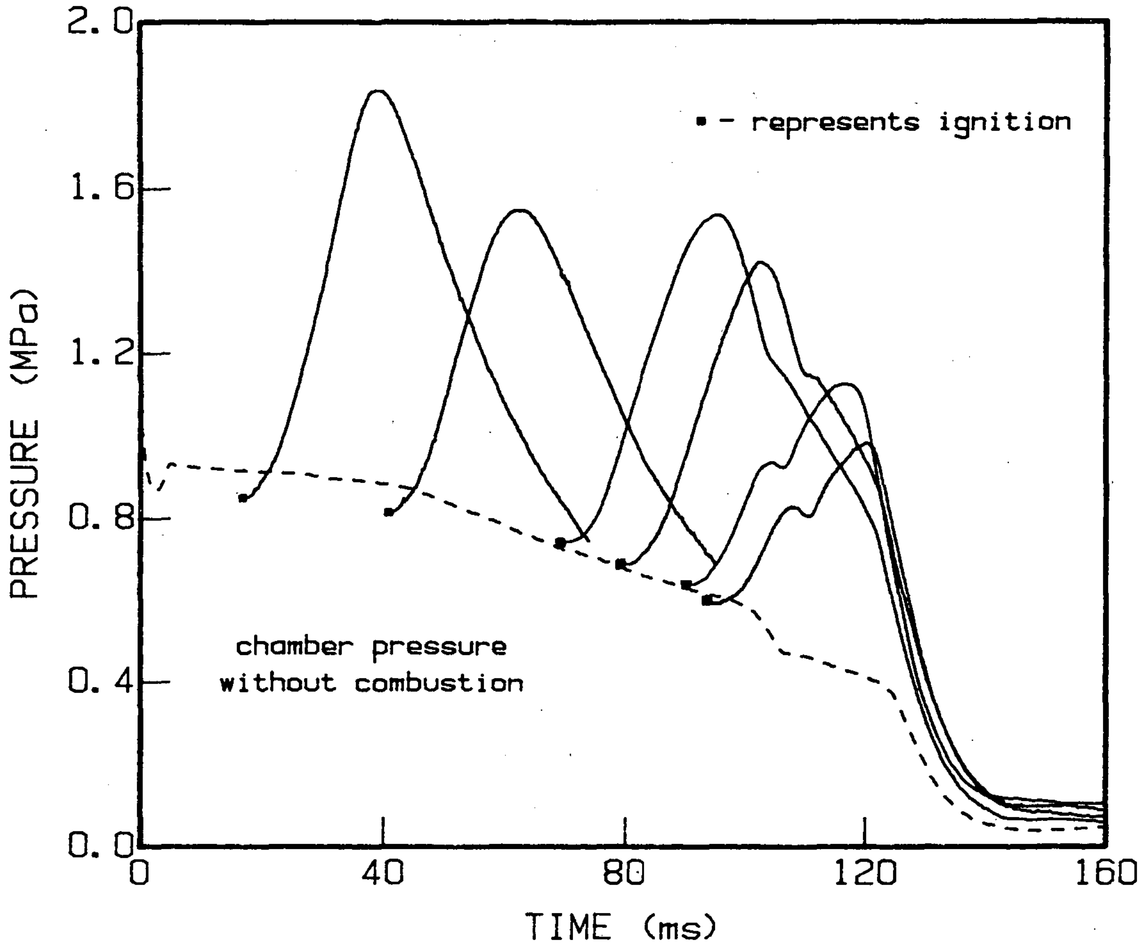

b) Peak pressure and time to peak pressure.

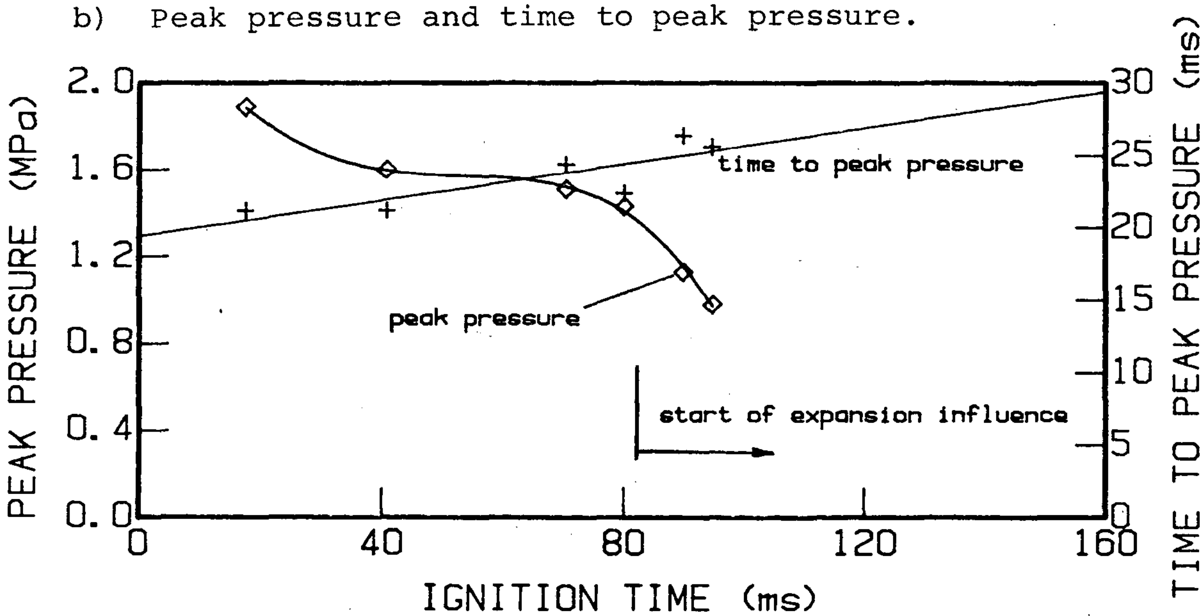

Figure 5. Effect of ignition time on chamber pressure, peak pressure, and time to peak pressure. Equivalence ratio = 0.65, compression time = 15 ms.

linearly with increasing ignition time indicating that the mass leak from the chamber is varying with time. There is a fast mass leak both during the primary compression and during the slow compression. Temperature measurements with a fine wire thermocouple (.013 mm, Type R) inside the compression chamber verify that up to 40% of the initial mass leaks out during the compression. After the piston reaches TDC the mass leak drops dramatically. This behavior is reflected in the peak pressure results.

Compression-Combustion: effect of equivalence ratio

Equivalence ratio is the most dominant factor in the time to peak pressure and peak pressure of compression-combustion events. Figure 6 shows the combustion at a single ignition time (80 ms) and a single compression time (15 ms) with various equivalence ratios (0.61, 0.65, 0.71, 0.76, 0.83, 0.88). Even at this long ignition time the flame shape development, Figure 6a, is nearly identical to the flame shape development with shorter ignition time, Figure 5a. Figure 6c reports the peak pressure and time to peak pressure as a function of equivalence ratio.

The peak pressure decreases linearly with equivalence ratio. A linear relationship between peak pressure and equivalence ratio is expected from available combustion energy considerations alone. This suggests that the effect of mass loss and heat transfer during the combustion is not significant.

The time to peak pressure increases linearly with

a) Typical flame propagation. t* = total combustion time.

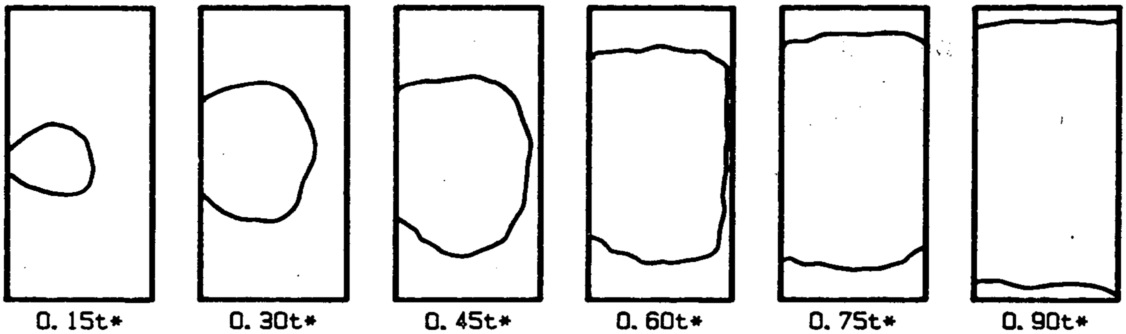

b) Chamber pressure for various equivalence ratios.

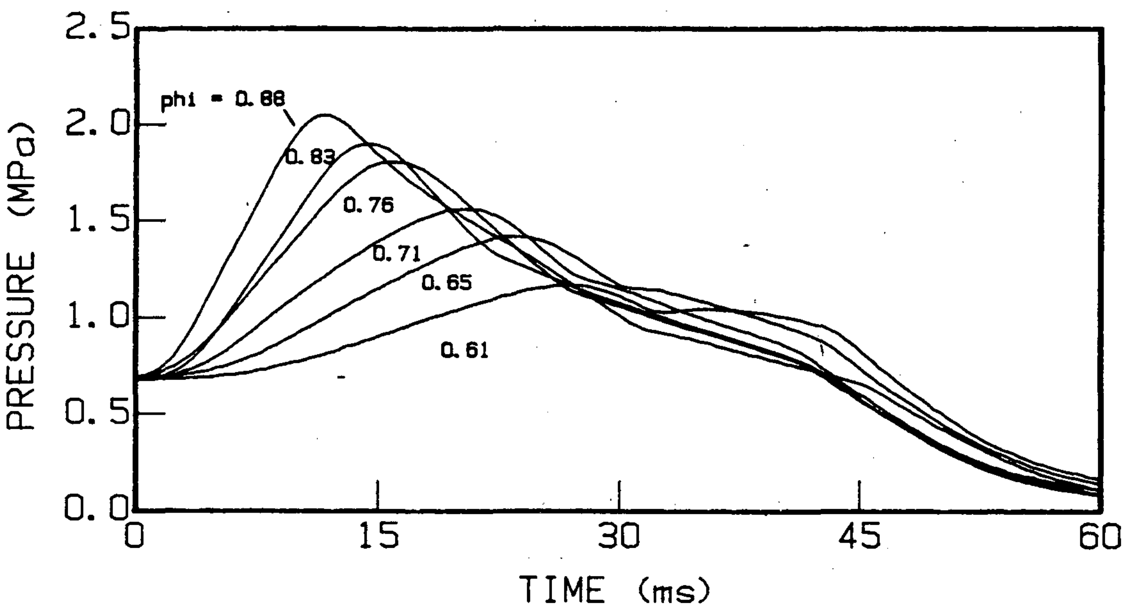

c) Peak pressure and time to peak pressure.

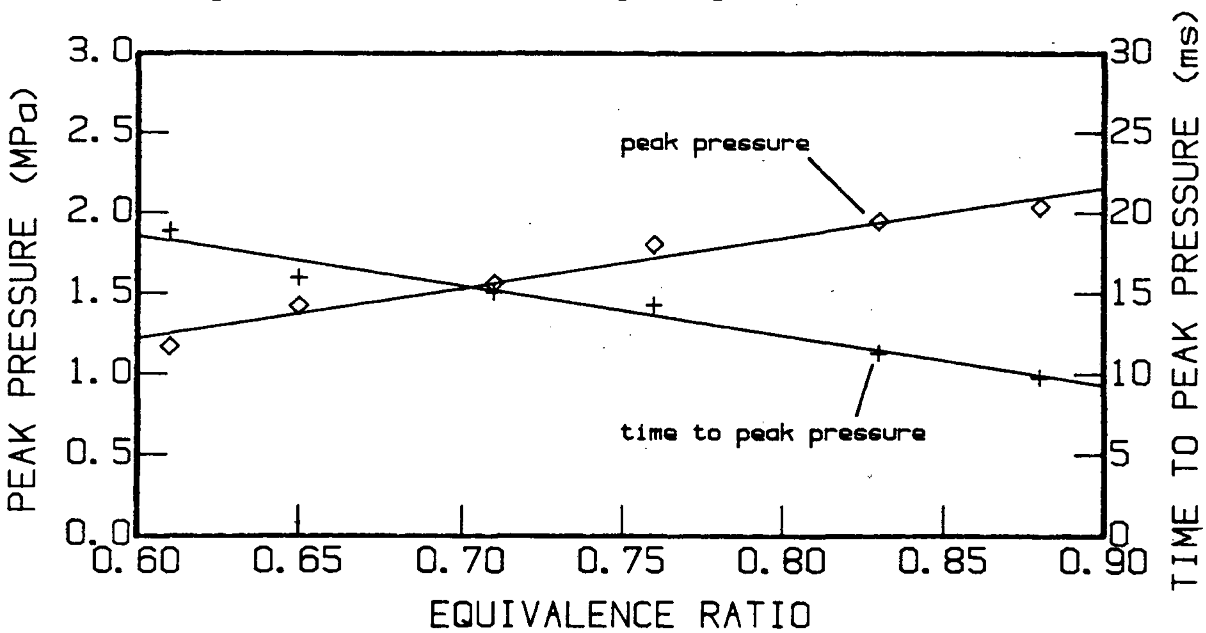

Figure 6. Effect of equivalence ratio in compression-combustion. Compression time = 15 ms, ignition time = 80 ms. phi denotes equivalence ratio.

decreasing equivalence ratio. The time to peak pressure increase with decreasing equivalence ratio is due to the decrease in laminar flame speed with decreasing equivalence ratio. Andrews and Bradley (1972) report that the laminar flame speed of methane-air mixtures is linearly decreasing with decreasing equivalence ratio from 0.9 to 0.60. Their data indicates an approximate halving of the flame speed over the equivalence ratio range from 0.83 to 0.61 (32.1 cm/s to 16.7 cm/s). The data of Figure 6c shows that the time to peak pressure is doubled over the equivalence ratio range from 0.83 to 0.61 (13.3 ms to 26.7 ms). The linear relationship between time to peak pressure and equivalence ratio, from the compression-combustion experiments, agrees very well with the linear relationship between the laminar flame speed and equivalence ratio reported by Andrews and Bradley.

COMPRESSION-EXPANSION-COMBUSTION

Experiments are conducted with flames ignited just before the expansion stroke of the rapid compression machine.

The effect of piston withdrawal on flame propagation is twofold. First, the expansion stretches the flame, creating a diverging flame front. Secondly, the expansion removes energy from the bulk burned and unburned gas.

The flame stretch phenomenon was characterized first by Karlovitz (1953) and later refined by Strehlow and Savage (1978). A divergent flame front must raise more preheat gases to ignition temperature at each time in the combustion.

If the divergence is great enough the energy liberated in the combustion is unable to elevate the preheat gases to ignition temperature and the flame is extinguished. The Karlovitz number, as defined by Strehlow and Savage (1978), is a measure of the net heat deficit of the diverging flame front,

$$K = \frac{d}{dt}\left[\log\ (\Delta A)\right] \frac{\eta}{S_u} \qquad (1)$$

The larger the Karlovitz number, the greater the heat deficit. S_u is the laminar flame speed. The logarithmic derivative term represents the fractional rate of flame area increase. This term is much larger for sections of the flame perpendicular to the piston face than it is for those sections parallel to the piston face. η is the width of the preheat zone and can be calculated from measurable data (Lewis and Von Elbe, 1961),

$$\eta = \frac{\alpha}{S_u} \qquad (2)$$

where α is the thermal diffusivity of the unburned gas. Replacing η in Equation 6 it is seen that the Karlovitz number is related to the inverse square of the laminar flame speed. The low flame speed of lean mixtures produce large Karlovitz numbers which suggests sensitivity to flame stretch effects. There is a critical Karlovitz number associated with flame extinguishment (Lewis and Von Elbe, 1961). The Karlovitz number of all flames in the compression-expansion-combustion experiments is below this critical extinguishment value. The flame stretch is responsible, however, for the reduction of the combustion rate in regions where the flame is perpendicular to the piston face.

The second effect of piston withdrawal is to remove energy from the entire bulk of working fluid. The energy removal appears as decreased burned and unburned gas temperature. It has been shown (Smith, Westbrook and Sawyer, 1979) that bulk quenching occurs when the expansion is sufficient to reduce the adiabatic flame temperature, based on the unburned gas properties, to approximately 1606 K. If the flame temperature falls below the critical value, there is insufficient reaction energy to raise the preheat gases to ignition temperature. The adiabatic flame temperature in the compression-expansion-combustion experiments is not below this critical value except for the leanest mixture tested (equivalence ratio 0.61).

Compression-Expansion-Combustion: calculation of mass burned

The simultaneous records of flame location and pressure allow calculation of the mass fraction burned at each stage in the combustion. High speed schlieren movies of the combustion process are used to measure the volume of burned gas. The image is assumed two-dimensional due to the line ignition flame initiation. The uncertainty in the unburned volume, due to poor flame definition, of expansion-combustion events starting with atmospheric initial conditions has been shown to be about 7% (Smith, 1977). In compression-expansion-combustion cases the uncertainty increases as the schlieren image loses clarity during the previously discussed piston bounce phenomenon. In compression-expansion-combustion cases the uncertainty in burned volume may be as large as 15%. With possible errors of this magnitude differential analyses leading to mass burning rates cannot be employed without a considerable amount of smoothing. Consequently, an integrated method is used.

Assumptions:

1) No net heat flux occurs across the boundaries of the unburned gases.

2) The flame front is negligibly thin

3) The unburned gas behaves as an inviscid ideal gas of constant constant composition corresponding to that of the initial mixture.

4) The pressure is spatially uniform inside the combustion chamber.

5) No mass loss from combustion chamber.

The acceptability of these assumptions (with the exception of assumption 5) has been demonstrated by Smith (1977). Assumption 5 is adopted because the relatively low pressure and short event duration of compression-expansion-combustion does not allow significant mass leak. The assumption is supported by the compression-combustion results reported earlier. The mass contained in the unburned gas is:

$$M_u = \frac{P*V_u}{R*T_u} \tag{3}$$

from the ideal gas relation. Using assumption 1) the unburned gas temperature may be expressed as the adiabatic compression temperature,

$$T_u = T_o * (\frac{P}{P_o})^{(\frac{\gamma-1}{\gamma})} \tag{4}$$

where γ is the ratio of specific heats for the unburned gas and the subscript o denotes initial values. Constant γ is assumed over the small temperature range of the unburned gas. Substituting Equation 2 into Equation 1 and recognizing the expression,

$$M_o = \frac{P_o * V_o}{R * T_o} \tag{5}$$

as the initial mass, the ratio of mass unburned to initial mass is given by:

$$\frac{M_u}{M_o} = \left(\frac{P}{P_o}\right)^{\left(\frac{1}{\gamma}\right)} * \left(\frac{V_u}{V_o}\right) \tag{6}$$

Using assumption 5) the ratio of the burned mass to the initial mass is:

$$\frac{M_b}{M_o} = 1 - \left(\frac{P}{P_o}\right)^{\left(\frac{1}{\gamma}\right)} * \frac{(V_t - V_b)}{V_o} \tag{7}$$

where V_t is the instantaneous volume of the chamber and V_b is the burned gas volume.

The burned volume and total volume of the chamber are determined from high speed schlieren movies. The flame is assumed two-dimensional. Burned area is determined using a planimeter on tracings of the flame shape. The burned volume is obtained by multiplying the burned area by the chamber depth. The total volume is computed from the piston location and the cross-section of the chamber.

<u>Compression-Expansion-Combustion: uncertainties</u>

The uncertainty in the pressure is negligibly small. The uncertainty in the calculated mass burned fraction is due to possible measurement errors in the burned volume and total volume. There is one uncertainty associated with the two-dimensional flame shape assumption. This uncertainty is only significant at the start of combustion. Once a plenum of burned gas has developed three-dimensional flame effects are small. The larger contribution to the uncertainty in the mass burned comes from the assumed flame location. When the flame is near the walls the finite thickness of the schlieren image makes determination of the exact flame and wall location difficult. For flames burning in greatly expanded volumes an absolute error of 2.5 mm in flame location could generate a 25% error in burned volume. The narrower flames with large surface to burned volume ratio are susceptible to the largest errors. The planimeter method of integration corrects somewhat for the flame location uncertainty, but the mass fraction burned can be expected to give only trends reliably.

Compression-Expansion-Combustion: results

The shapes of flames ignited just before the expansion stroke are summarized for various equivalence ratios (0.61, 0.65, 0.71, 0.76, 0.83, 0.88) in Figure 7. The flame growth in regions perpendicular to the piston face are noticeably retarded by the piston induced flame stretch. The effect is particularly noticeable in the leaner flames (equivalence ratio 0.61, 0.65, 0.71). The low equivalence ratio flames are significantly narrower than the higher equivalence ratio flames. Flames burning during expansion exhibit three basic

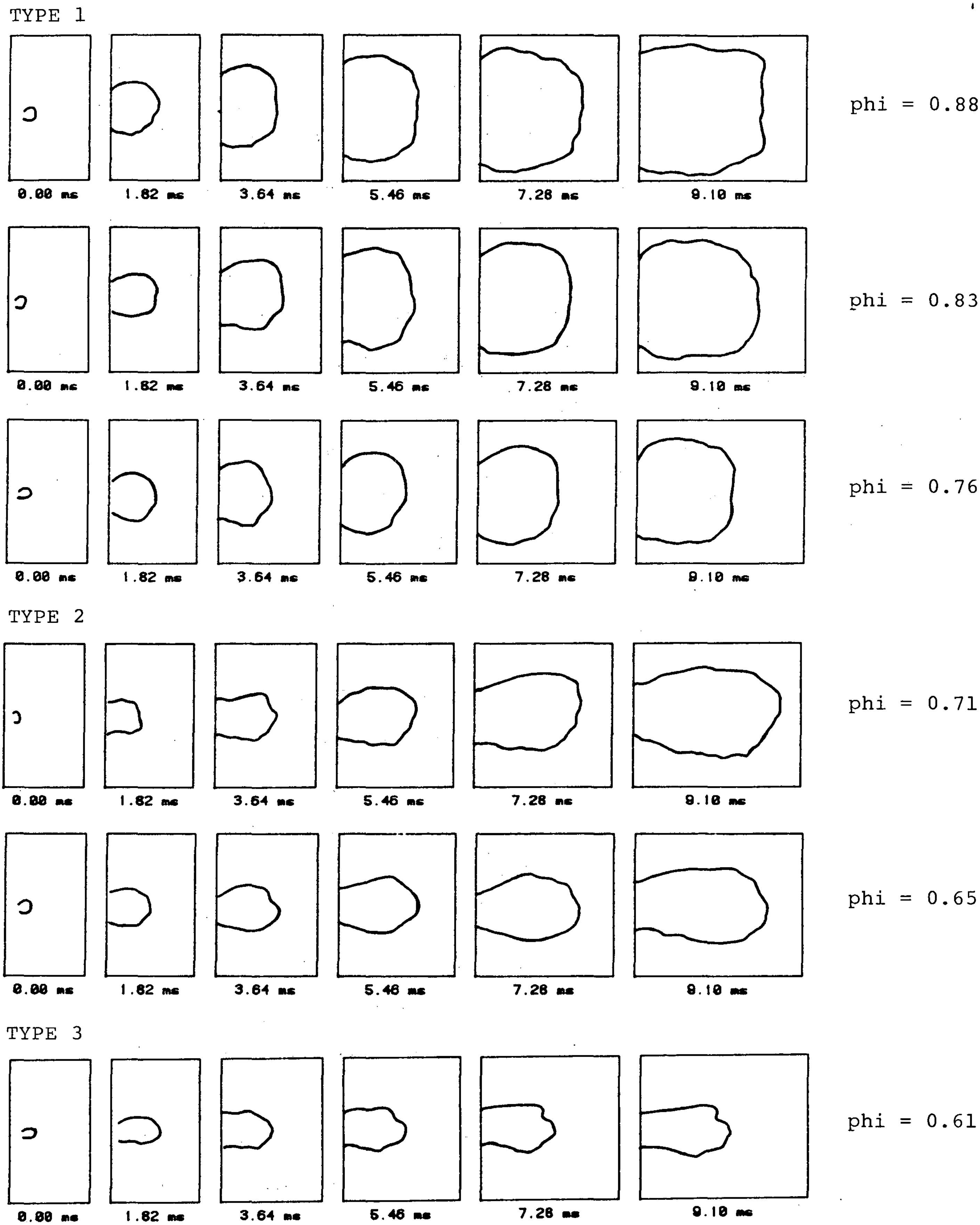

Figure 7. Flame propagation in compression-expansion-combustion for various equivalence ratios. phi denotes equivalence ratio.

behaviors: Type 1) For higher equivalence ratios the flames burn fast enough to catch up to the expanding piston and burn the entire mixture before the expansion is concluded. Type 2) The combustion of the middle equivalence ratios begins during the early part of the expansion. When the expansion velocity becomes large the burning rate decreases. Once the piston is fully expanded the combustion rate increases again and the final gases are combusted at constant volume. Type 3) The near ignition limit flame begins to burn during the early part of the expansion. Once the piston moves rapidly the burning rate drops to zero. The burning rate never increases, that is, the flame is quenched. The three types of combustion are clearly observed from the pressure histories of the combustion events, Figure 8.

Type 1 (equivalence ratios 0.88, 0.83, 0.76):

Pressure, mass burned fraction and chamber volume fraction as functions of time for three equivalence ratios are shown in Figures 9a, b and c. The pressure curves consist only of the points used in the mass fraction burned calculation. Even this small number of points represents the pressure behavior satisfactorily. The mass burned points are fitted with a least squares linear regression line with the first few points excepted. The volume fraction points are fitted with a hand drawn smooth curve. There is considerable scatter in the mass fraction burned data, but a linear regression line, excepting the early points, does a fair job of approximating the trends. The pressure peak occurs at

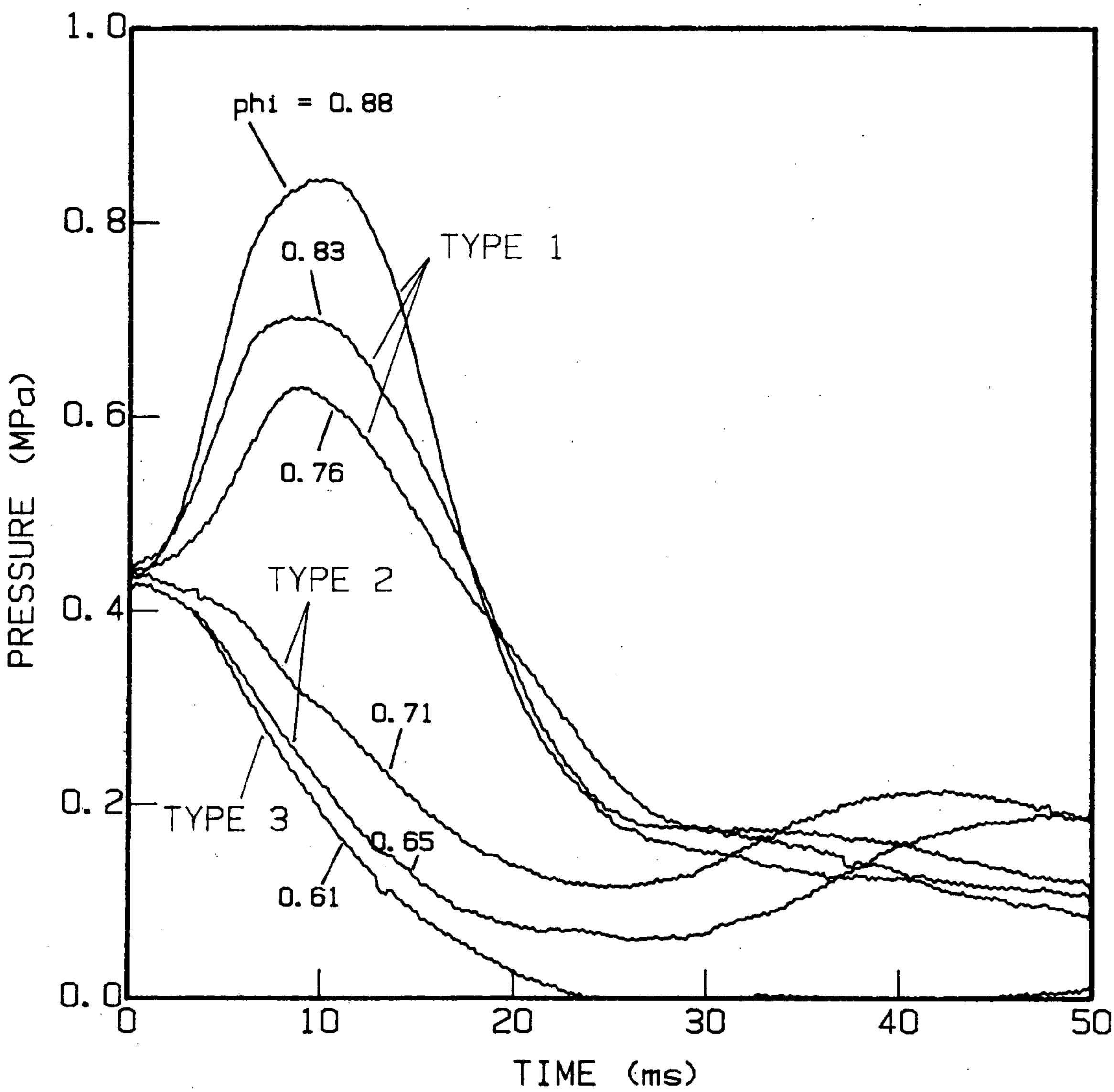

Figure 8. Chamber pressure in compression-expansion-combustion for various equivalence ratios. phi denotes equivalence ratio.

a) Equivalence ratio = 0.88.

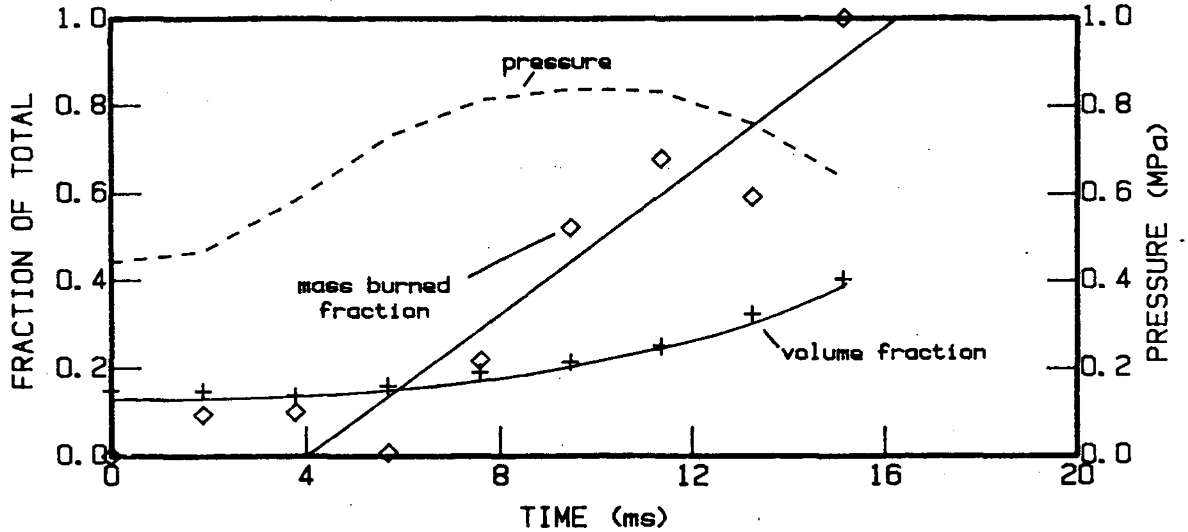

b) Equivalence ratio = 0.83.

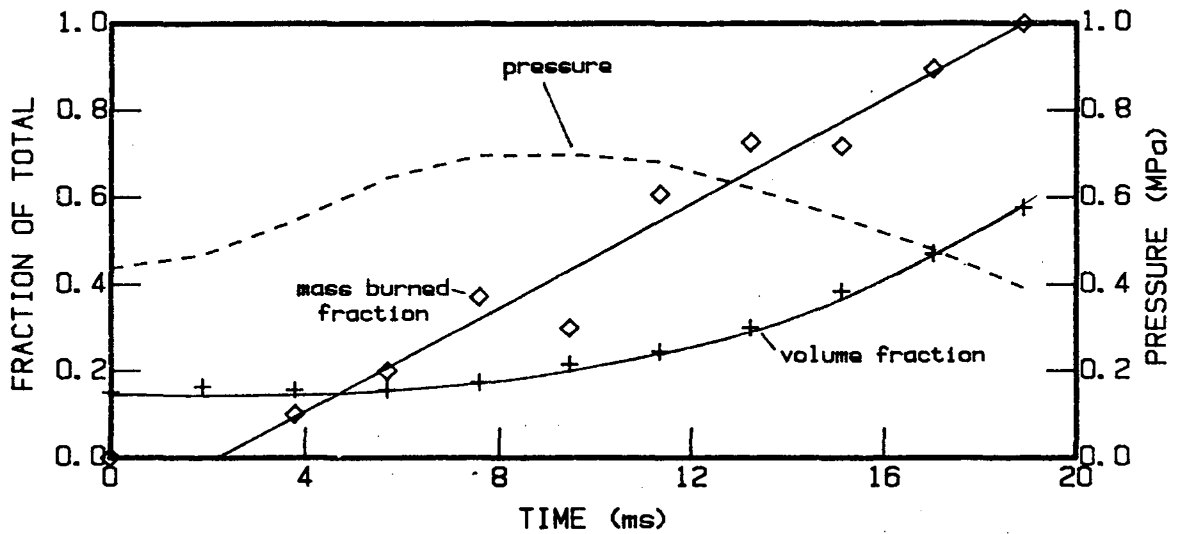

c) Equivalence ratio = 0.76.

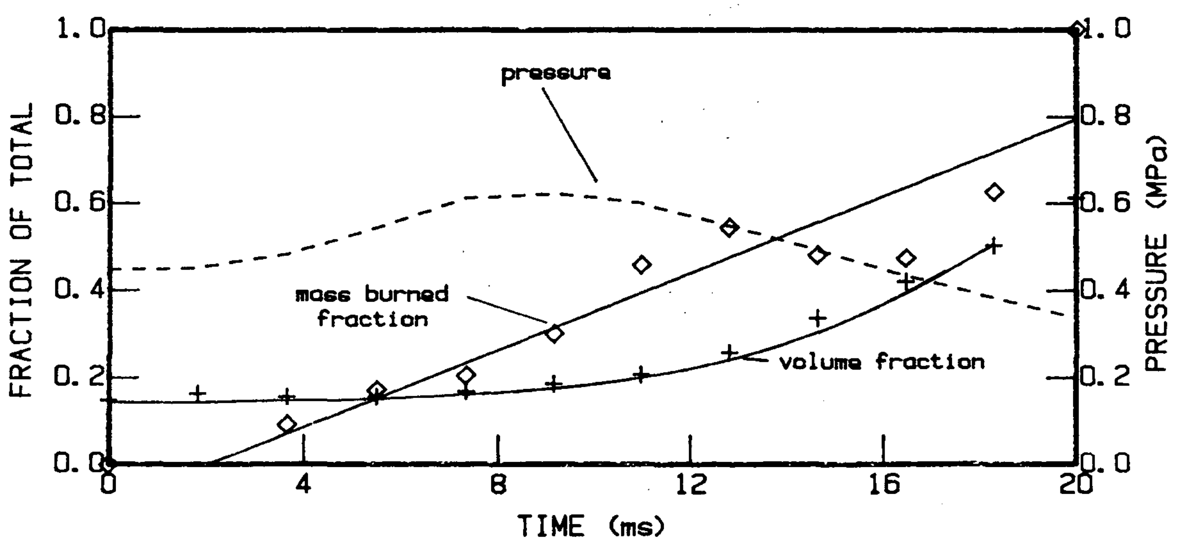

Figure 9. Pressure, mass burned fraction $\left(\frac{\text{mass burned}}{\text{initial mass}}\right)$, volume fraction $\left(\frac{\text{chamber volume}}{\text{maximum volume}}\right)$. Type 1 compression-expansion-combustion.

nearly the same time in all cases and the maximum pressure decreases with equivalence ratio, Figure 10a. The peak pressure occurs before the mixture is completely burned. This indicates that the removal of energy by the piston motion exceeds the energy input from the combustion at nearly the same time in the stroke. The pressure peaks are considerably more rounded for compression-expansion-combustion than for compression-combustion, Figure 6.

The mass burned fraction starts off slowly and then increases approximately linearly with time, Figure 10b. All of the Type 1 flames consume a significant fraction of the mass (20%) in less than 8 ms. The flames pass the 20% mass burned threshold before the chamber volume has noticeably increased. Linear mass burned fraction represents constant mass burning rate. During the linear portion of the mass fraction burned curves the mass fraction burning rate is computed for each of the three equivalence ratios. The function of mass fraction burning rate versus equivalence ratio closely matches the function of laminar flame speed versus equivalence ratio obtained by Andrews and Bradley (1972), Figure 10c. This indicates that the difference in mass burning rate for the different equivalence ratio flames can be attributed almost entirely to the effect of equivalence ratio on the laminar flame speed. The definition of the mass burning rate is taken to be:

$$\dot{M} = \rho S_u A_f \qquad (8)$$

where S_u is the laminar flame speed, ρ is the density of

a) Peak pressure and time to peak pressure.

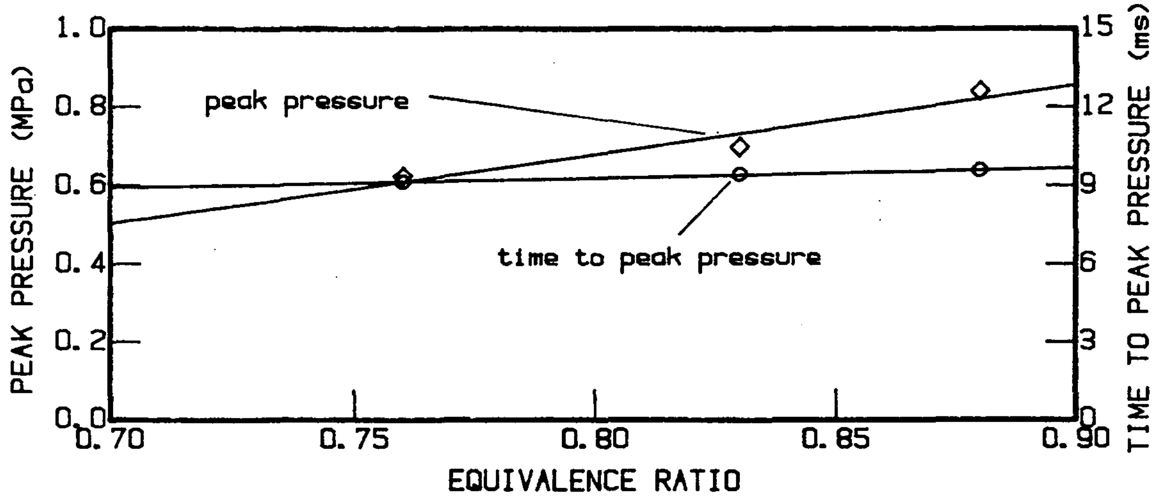

b) Mass fraction burned.

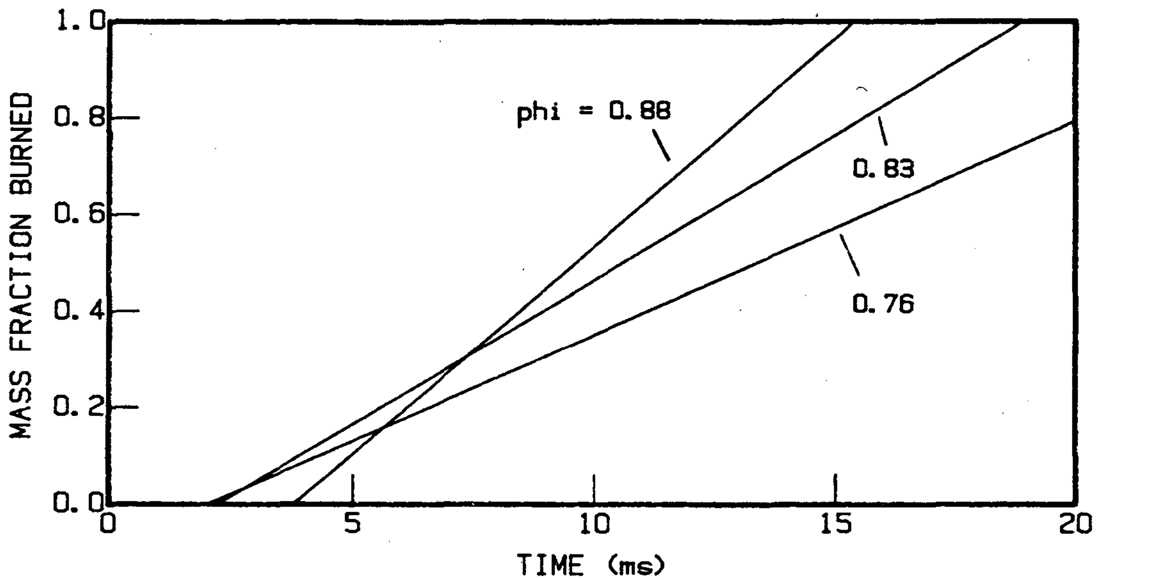

c) Burning rate and flame speed.

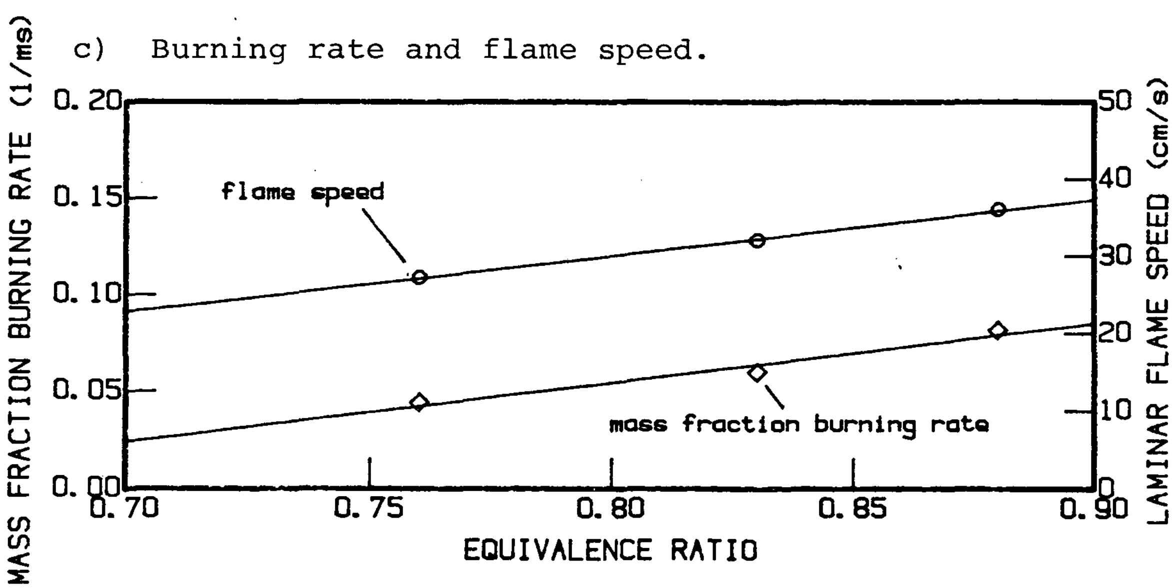

Figure 10. Type 1 combustion summary.
Flame speed results from Andrews and Bradley (1972).

the unburned mixture, and A_f is the flame area. Andrews and Bradley (1972) report a laminar flame speed correlation function for methane-air mixtures. The function indicates that the laminar flame speed is nearly constant for adiabatic compression and expansion. Hence, for constant mass burning rate, the product of ρ and A_f would also have to be a constant. This is clearly not true in the reported cases. Both the flame area and the density are increasing for much of the combustion. It is probable that the chamber walls affect significantly the flame speed.

Type 2 (equivalence ratios 0.71, 0.65):

The results for the middle equivalence ratios tested are shown in Figure 11. The pressures are slightly higher than the pressure with no combustion and exhibit a minimum which corresponds to the time when the piston slows its expansion.

The mass fraction burned points are fit with hand drawn smooth curves. The curves indicate two combustion events. The first follows ignition and develops as the combustion of higher equivalence ratio mixtures develop. The flame is then stretched by the piston movement and the burning of flame sections parallel to the side walls is reduced dramatically. During this period the mass fraction burned curvature changes sign. This represents a decrease in mass burning rate. The adiabatic flame temperature is not below the 1606 K figure required for bulk quenching to occur. Once the piston slows, the combustion rate begins to increase. The combustion in this phase occurs at virtually constant expanded volume. The

a) Equivalence ratio = 0.71.

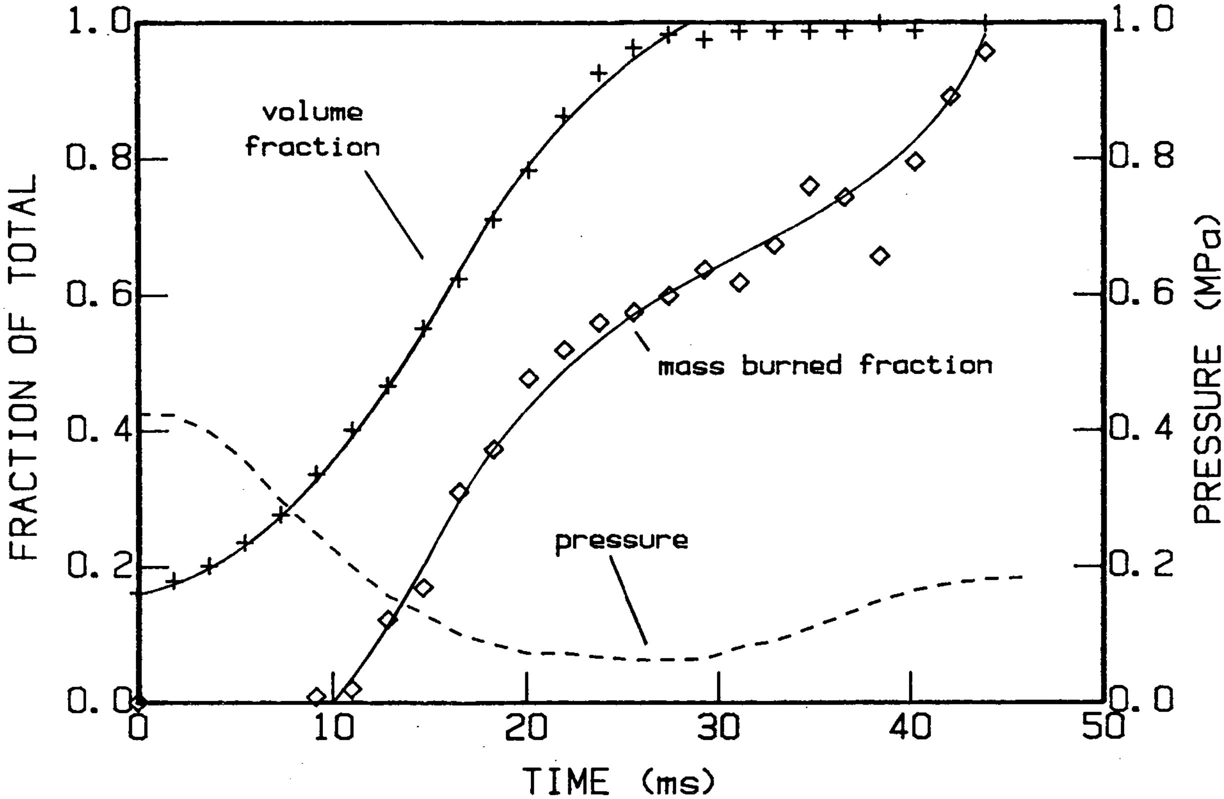

b) Equivalence ratio = 0.65.

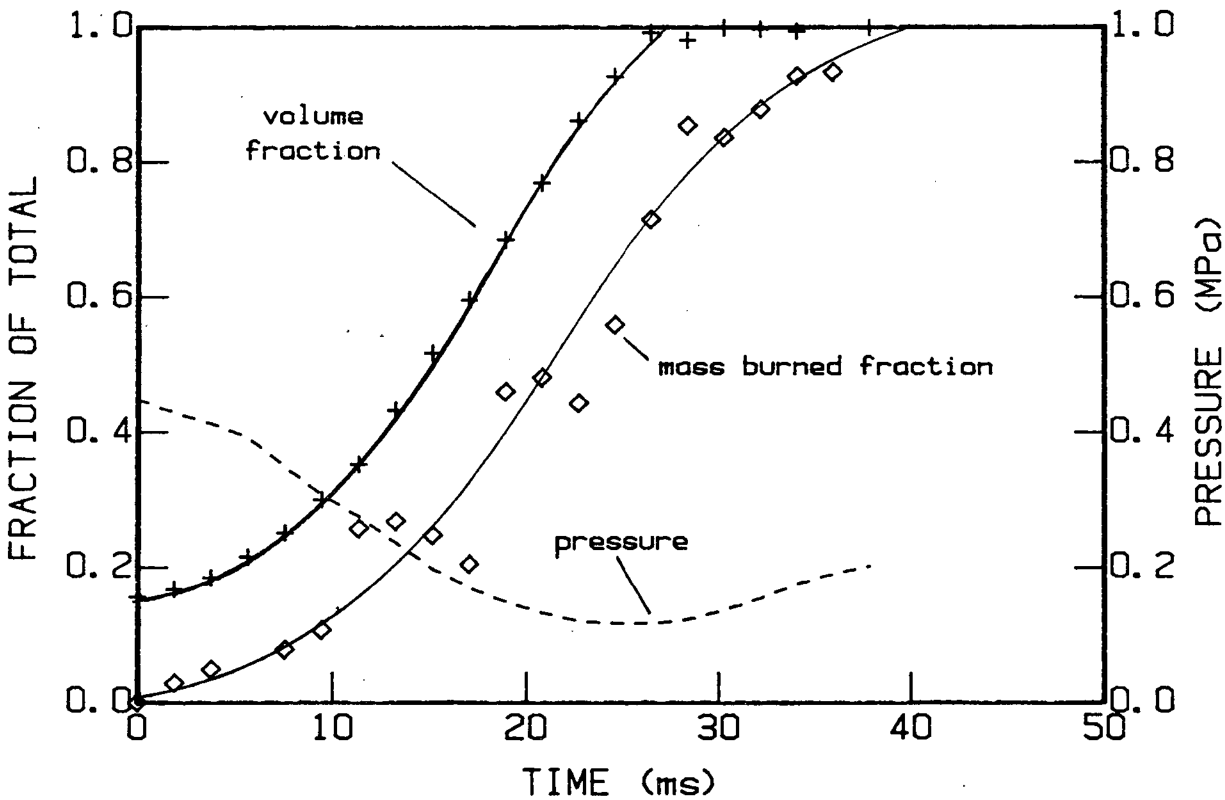

Figure 11. Pressure, mass burned fraction $\left(\frac{\text{mass burned}}{\text{initial mass}}\right)$, volume fraction $\left(\frac{\text{chamber volume}}{\text{maximum volume}}\right)$. Type 2 compression-expansion-combustion.

final stages of the constant volume combustion phase is characterized by formation of a tulip shaped flame. The formation of a tulip flame during constant volume flame propagation in closed vessels has been noted by many other experimenters (Lewis and Von Elbe, 1961, Guenoche, 1964, Woodard et al., 1981, Steinert et al.,1982). For Type 2 combustion the significant mass fraction burned point is not reached until the piston is well underway.

Type 3 (equivalence ratio 0.61):

The pressure in quenched combustion is essentially identical to the pressure without combustion, Figure 12a. The mass fraction burned initially behaves as the mass fraction burned curves of Type 2 flames, Figure 12b. Further into the combustion the lower equivalence ratio, Type 3, flame cannot generate enough heat during the expansion process to make up for the energy removed by the piston motion. Consequently, when the piston reaches the halfway point the flame is quenched. The quench process is likely to be due to bulk quench as the adiabatic flame temperature of the unburned mixture is below 1600 K at the quench time. The volume ratio at quenching is defined by Smith (1977),

$$\Theta = \frac{(V - V_o)}{V_o} \tag{9}$$

where V is the chamber volume and V_o is the initial volume. The volume ratio at quenching for the 0.61 equivalence ratio flame is 1.77. This result agrees very well with the results obtained by Smith (1977) for laminar expansion-combustion

a) Chamber pressure with and without combustion.

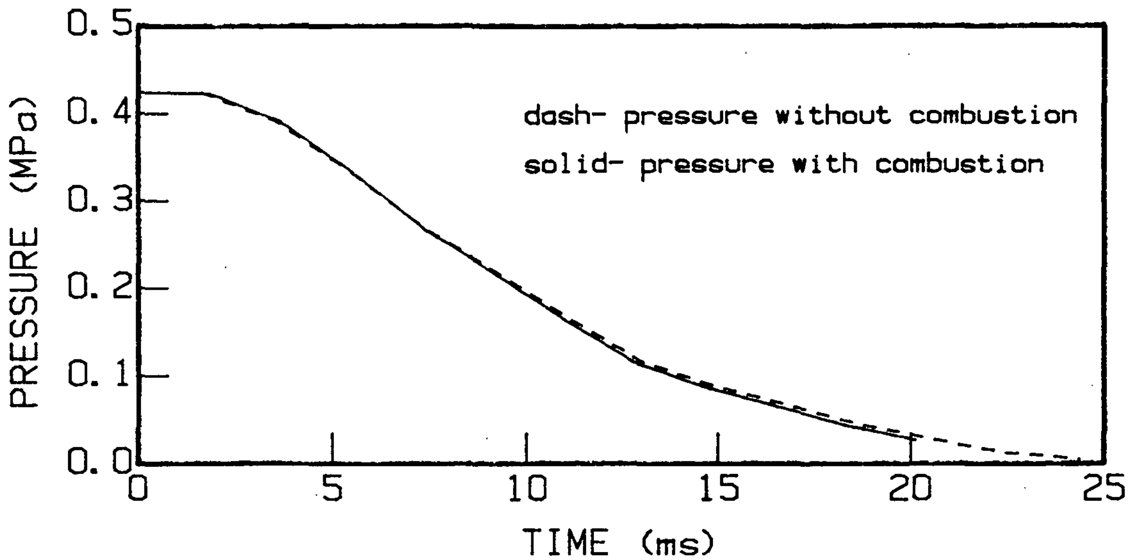

b) Equivalence ratio = 0.61. X indicates quench.

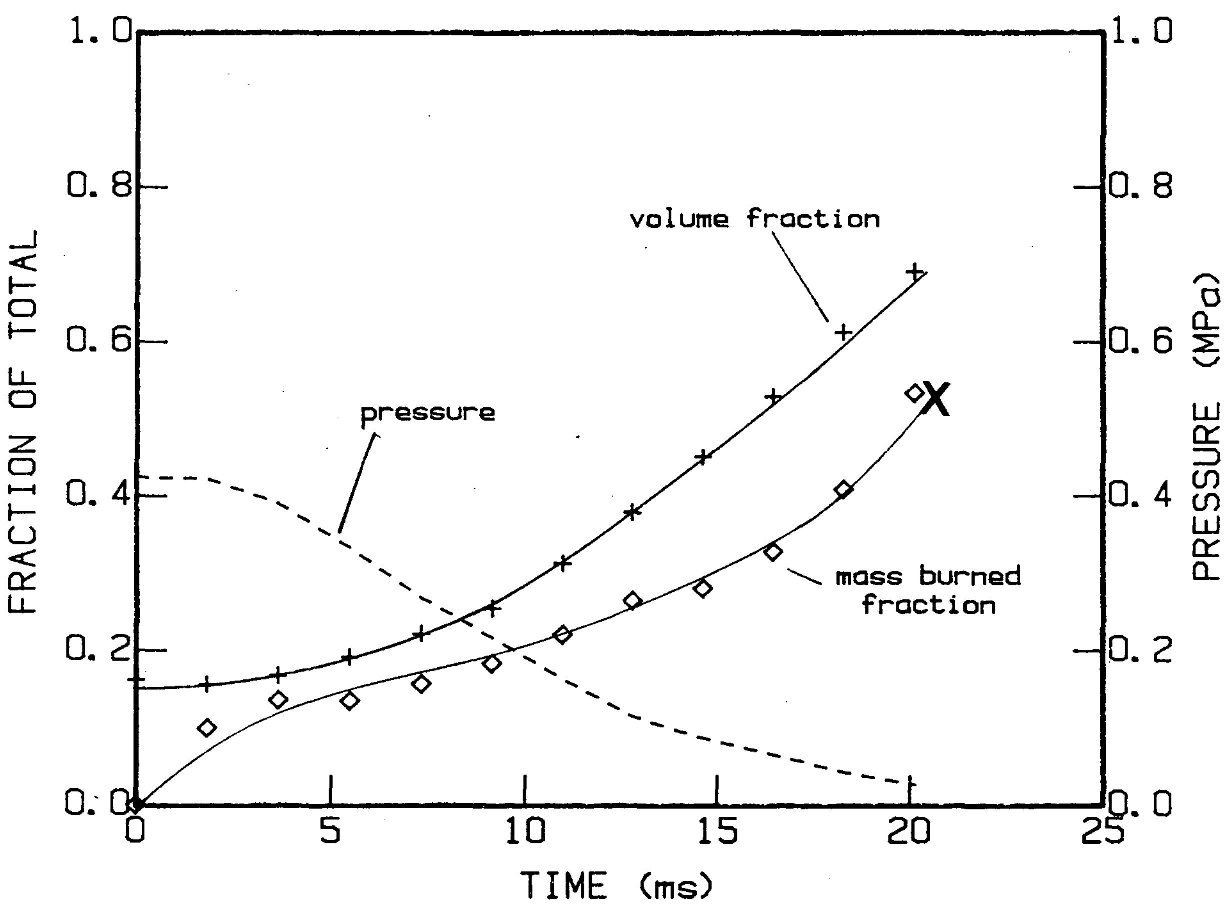

Figure 12. Pressure, mass burned fraction $\left(\frac{\text{mass burned}}{\text{initial mass}}\right)$, volume fraction $\left(\frac{\text{chamber volume}}{\text{maximum volume}}\right)$. Type 3 compression-expansion-combustion.

without initial compression.

Compression-Expansion-Combustion: observations

The behavior of flames burning in the expansion is critically related to the equivalence ratio. There appears to be a critical equivalence ratio which changes the flame propagation from Type 1 to Type 2 combustion. The limited accuracy of the mixture ratio makes this critical equivalence ratio difficult to predict precisely but it lies between 0.71 and 0.76. Figure 13a presents the mass burned fraction versus time for the five complete burning flames (equivalence ratio 0.65, 0.71, 0.76, 0.83, 0.88). Smooth curves are drawn through the data to help identify each case. Figure 13b shows the mass burned fraction versus volume ratio fraction. The separation between Type 1 and Type 2 combustion is represented by the line through the graph. There is a fair amount of scatter in the data but the distinction between Type 1 and Type 2 combustion is clear. In Type 1 combustion half of the mass is burned during the first tenth of the expansion. Type 2 combustion is characterized by minimal mass burned during the initial expansion phase and a large fraction of the mass burned at expanded volume. It appears that rapid early combustion is critically important to insure complete combustion during expansion.

CONCLUSIONS

A study is made of flames propagating in a rapid compression, expansion machine. Simultaneous high-speed

a) Mass burned fraction versus time.

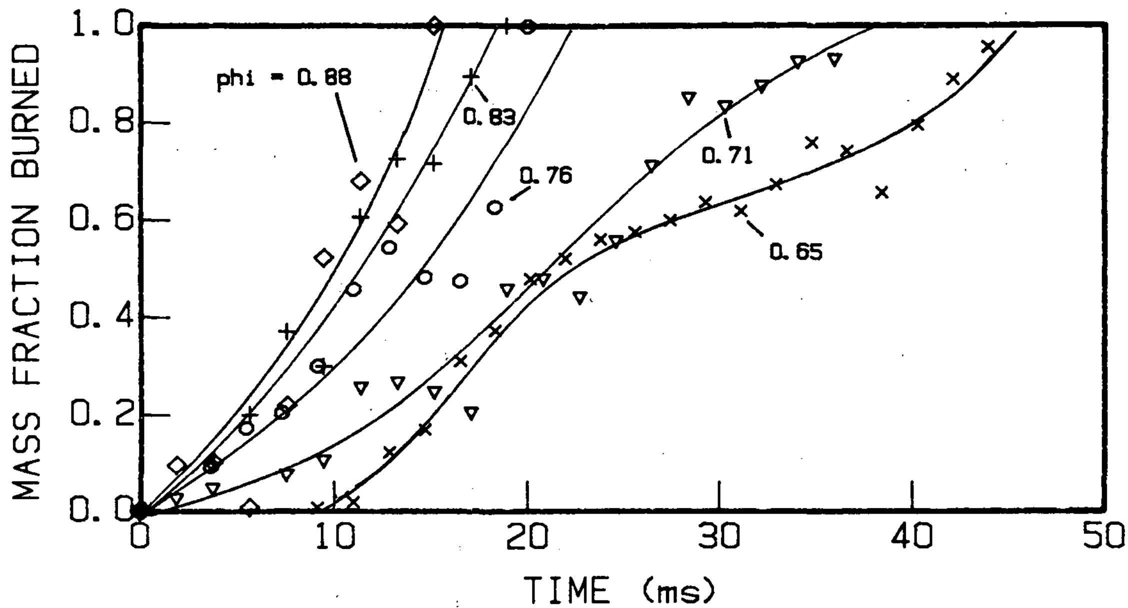

b) Mass burned versus volume fraction.

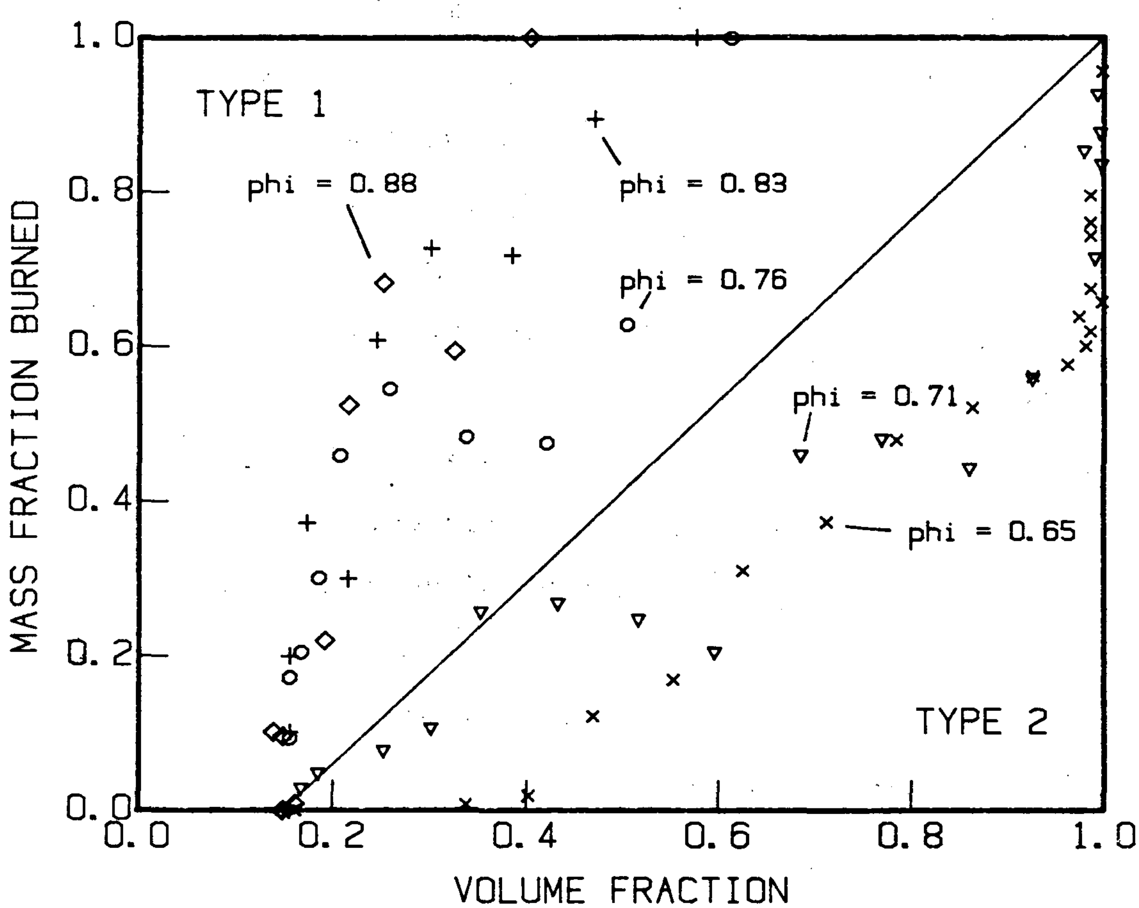

Figure 13. Mass burned fraction in compression-expansion-combustion for various equivalence ratios. phi denotes equivalence ratio.

schlieren movies and pressure measurements are taken. From these data mass fraction burned information is extracted. Two combustion situations are investigated. 1) Compression followed by combustion at compressed volume, 2) Compression, expansion with combustion occurring during the expansion stroke.

Compression-combustion experiments indicate that the equivalence ratio is almost entirely responsible for the variations in burning time and peak pressure. This result suggests a negligible contribution of the piston generated fluid motion to the combustion.

Compression-expansion-combustion experiments show a distinct bifurcation in flame behavior. Above a critical equivalence ratio, about 0.73, the flame burns faster than the piston expansion and the mixture is burned before the piston comes to rest. Below this critical value the flame is arrested at some point during the piston expansion. After the piston slows near the end of its expansion the flame begins to propagate again, burning the remainder of the mixture. Above the critical equivalence ratio the mass burning rate is approximately constant after the initial flame development period. The constant mass burning rate depends nearly linearly on equivalence ratio. Below the critical equivalence ratio the piston dominates the event. Once the piston reaches its rest point the combustion is a constant volume process.

Bulk quenching was observed only for the leanest mixture tested.

ACKNOWLEDGEMENTS

The authors appreciate the extensive assistance provided by Ken Hom in the preparation of the apparatus. Gary Hubbard developed much of the data logging software. This work was supported by the Assistant Secretary for Conservation and Renewable Energy, Office of Transportation Programs, Division of Transportation Energy of the U.S. Department of Energy under contract number DE-AC03-76SF00098.

REFERENCES

Andrews, G.E., Bradley, D. (1972). The burning velocity of methane-air mixtures. Combustion and Flame, 19, 275-288.

Dale, J.D., Oppenheim, A.K. (1982). A rationale for advances in the technology of I.C. engines. SAE Paper No. 820047.

Guenoche, H., (1964). Flame propagation in tubes and in closed vessels. In Non-Steady Flame Propagation, G. Markstein (Editor), Pergamon Press, New York.

Karlovitz, B., Denniston Jr., D.W., Knapschaefer, D.H., Wells, F.E. (1953). Studies on turbulent flames, flame propagation across velocity gradients. Fourth Symposium (International) On Combustion, 229, Williams and Wilkins, Baltimore.

Lewis, B., Von Elbe, G. (1961). Combustion, Flames and Explosions of Gases, Chapter 5, Section 5 and 10. Academic Press, New York.

Matekunas, F.A. (1978). A schlieren study of combustion in a rapid compression machine simulating the spark ignition engine. General Motors Research Laboratory Report GMR-2770. Presented at the Seventeenth Symposium on Combustion, University of Leeds, England. August 20-25.

Noguchi, M., Landa, L., Nakamura, N. (1976). Development of the Toyota lean burn engine. SAE Paper No. 760757, SAE Transactions 1976, Section 4.

Oppenheim, A.K., Cheng, R.K., Teichman, K., Smith, O.I., Sawyer, R.F., Hom, K., Stewart, H.E. (1976). A cinematographic study of combustion in an enclosure fitted with a reciprocating piston. In Stratified Charge Engines, Institution of Mechanical Engineers Conference Publications 1976-11, 127-135.

Shiomoto, G.H., Sawyer, R.F., Kelly, B.D. (1978). Characterization of the lean misfire limit. SAE Paper No. 780235.

Smith, O.I. (1977). Lean limit combustion in an expanding chamber. Lawrence Berkeley Laboratory Report No. LBL-6851, PhD Thesis.

Smith, O.I., Westbrook, C.K., Sawyer, R.F. (1979). Lean limit combustion in an expanding chamber. Seventeenth Symposium (International) on Combustion, 1305-1313. The Combustion Institute, Pittsburgh.

Steinert, W., Dunn-Rankin, D., Sawyer, R.F. (1982). Influence of chamber length and equivalence ratio on flame propagation in constant volume duct. Western States Section/The Combustion Institute Paper No. 82-52 and Lawrence Berkeley Laboratory Report No. LBL-14965.

Strehlow, R.A., Savage, L.D. (1978). The concept of flame stretch. Combustion and Flame, 31, 209-211.

Woodard, J.B., Hirvo, D.H., Greif, R., Sawyer, R.F. (1981). Wall heat transfer and flame propagation in a constant volume duct. Western States Section/ The Combustion Institute Paper No. 81-51 and Lawrence Berkeley Laboratory Report No. LBL-13201.